Dynamic Analysis of Lateral Flow of Liquefied Ground

Ikuo Towhata
Professor of Civil Engineering, University of Tokyo

and

Hirofumi Toyota
Graduate Student, University of Tokyo

ABSTRACT

A theory of dynamic analysis was derived in order to make it possible to follow the time history of lateral ground motion triggered by seismic liquefaction. This theory obtains a single-degree-of-freedom differential equation, by solving which the time history is calculated. Since the equation have a viscous term and a residual strength that need a detailed study to understand, model shaking tests were performed. Those tests revealed that liquefied sand has a rate-dependent nature that is viscous as well as that the magnitude of the residual strength of liquefied sand is strongly affected by the presence of inertia force. Consequently, several cases were analyzed and compared with observation. Their agreement seems to be good.

INTRODUCTION

The lateral displacement of liquefied sandy ground has been analyzed by a variety of method. Since the damage to pipelines caused by this displacement is induced by the deformation of ground, whether compression or extension, the tool of displacement prediction is required to calculate the ground deformation. Therefore, an analysis on a rigid-block movement, in which there is no deformation, is not very suitable. A finite element analysis that features nonlinear stress-strain behavior of sand, development of excess pore water pressure, dynamic response of ground, and large deformation seems to be more useful. However, an analysis of this type requires a heavy computer duty. In this regard, Towhata et al. (1992) developed a closed-form solution of ground displacement.

The closed-form solution gave the ultimate displacement of ground that is associated with the minimum potential energy of ground and is possible to be reality only when the state of flow continues for a sufficiently long time. In contrast, shaking table tests (Toyota and Towhata, 1994) demonstrated that the state of flow is ceased when shaking ends. Only exception is a very loose sand that can continue to flow after shaking under the effects of gravity force. Consequently, it was found that the predicted displacement is greater than those observed in the field after earthquakes (Towhata et al., 1992)

The present study aims at a development of dynamic analysis that can trace the time-development of ground displacement during and after liquefaction. Since the original theory was closed-form, the present dynamic analysis was desired to be closed-form as well.

THEORY OF DYNAMIC ANALYSIS

Shaking table tests by Toyota and Towhata (1994) revealed that the lateral movement of liquefied ground is associated with a large shear deformation of soil in place of a rigid-block movement. The variation of lateral displacement in the vertical (z) direction is reasonably approximated by a sinusoidal function. Accordingly, the lateral displacement of ground, "u", at a location of (x,z) and at time "t" is expressed by

$$u(x,z,t)=\lambda(t)U(x,z) \tag{1}$$

in which x and z are horizontal and vertical coordinates respectively. U(x,z) is the ultimate displacement that would occur after a sufficiently long period of flow As illustrated in Fig.1, the effects of x and z components are separated from the time variation denoted by λ. Since U is able to be predicted by a closed-form solution (Towhata et al., 1992), the present study is

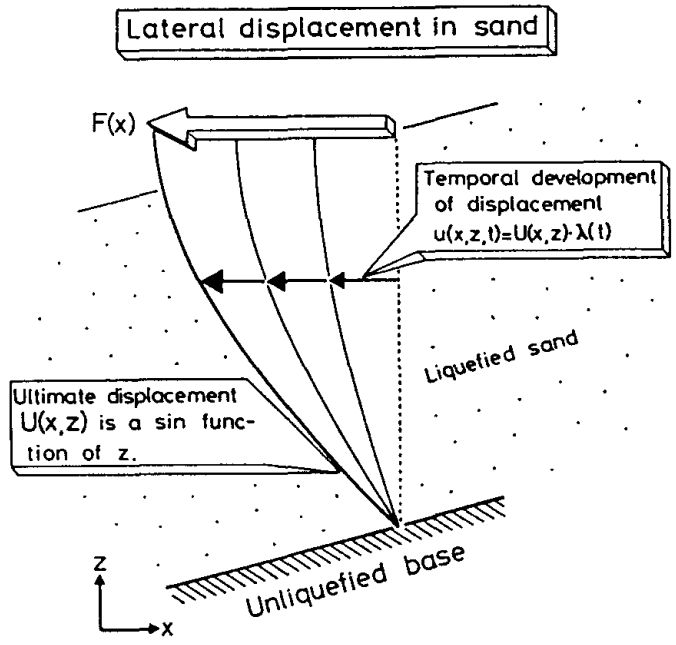

Fig.1 Modeling development of displacement with time.

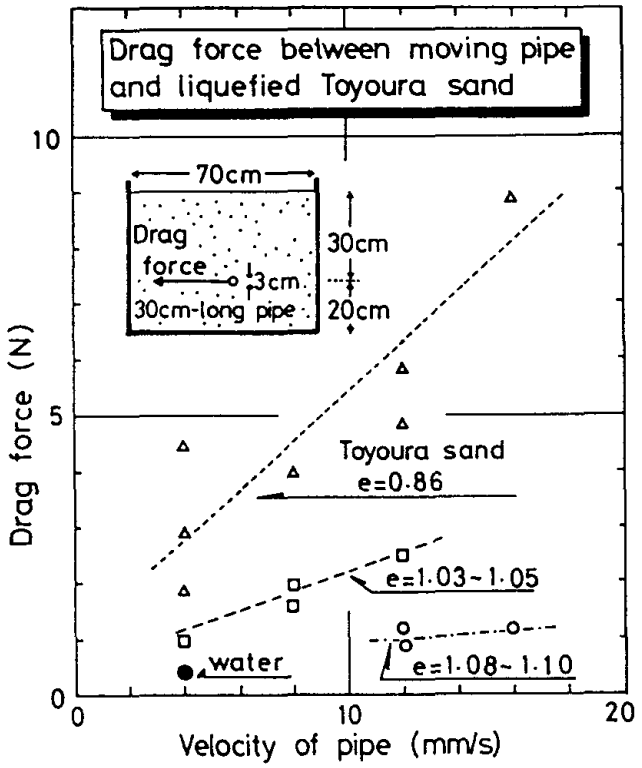

Fig.2 Rate-dependent nature of liquefied sand (Vargas, 1994).

focused on the derivation of $\lambda(t)$, a function of time.

The vertical displacement at time "t" is similarly expressed in terms of λ and W(x,z) that would occur after a sufficiently long period of flow;

$$w(x,z,t)=\lambda(t)W(x,z) \tag{2}$$

where W(x,z) was obtained by a closed-form solution (Towhata et al. 1992).

The velocity of ground is expressed by λ, U, and W;

$$\frac{\partial u}{\partial t}=U\frac{d\lambda}{dt} \quad \text{and} \quad \frac{\partial w}{\partial t}=W\frac{d\lambda}{dt} \tag{3}$$

The strain of soil is expressed similarly;

$$\varepsilon_x=\frac{\partial u}{\partial x}=\lambda\frac{\partial U}{\partial x} \qquad \varepsilon_z=\frac{\partial w}{\partial z}=\lambda\frac{\partial W}{\partial z} \quad \text{and}$$
$$\gamma=\frac{\partial u}{\partial z}+\frac{\partial w}{\partial x}=\lambda\left(\frac{\partial U}{\partial z}+\frac{\partial W}{\partial x}\right) \tag{4}$$

By using Eqs.3 and 4, it is possible to calculate the kinematic and the potential components of energy of ground at any x and z. The energy is thereafter integrated all over the ground to derive the global energy components, denoted by K and Q. Note that the kinematic energy, K, consists of $d\lambda/dt$ while the potential energy, Q, is composed of λ.

K and Q as derived above were substituted in the Lagrangean equation of motion;

$$\frac{d}{dt}\left\{\frac{\partial(K-Q)}{\partial(\partial\lambda/\partial t)}\right\}-\frac{\partial(K-Q)}{\partial\lambda}=0 \tag{5}$$

Consequently, a single-degree-of-freedom equation of motion in terms of λ was derived,

$$m\frac{d^2\lambda}{dt^2}+k\lambda=k \tag{6}$$

Eq.6 shows that the static equilibrium occurs at $\lambda=1$ that means u=U.

Earlier, the liquefied soil was considered to be of zero shear stiffness and constant volume, similar to liquid. Moreover, the unliquefied dry layer at the surface was regarded as an elastic column that resists against lateral compression. Accordingly, the initial analyses were carried out by using Eq.6. However, the results were poor because Eq.6 gives a free oscillation without damping, which is hardly the case in reality The rate of displacement was found to be much faster than observed in tests. Furthermore, the equation could not reproduce the experimental fact that a ground of a slightly higher density stops movement when the surface is still inclined, probably due to some shear resistance at large deformation. Thus, two more terms were added to Eq.6;

$$m\frac{d^2\lambda}{dt^2}+c\frac{d\lambda}{dt}+k\lambda=k-r\tau_r \tag{7}$$

The second term added to the left-hand side stands for viscosity and the last term on the right-hand side indicates the contribution from a residual strength of sand at large distortion.

SIGNIFICANCE OF VISCOSITY TERM

It appears necessary to examine the viscous nature of liquefied sand as included in Eq.7, because liquefied sand consists of sand grains and pore water both of which have no viscous characteristics. For this purpose, model shaking tests were conducted in which a pipe embedded in a liquefied sand was pulled laterally. The drag force needed for a constant-velocity movement of the pipe was recorded together with the pipe velocity so that the rate-dependent nature of the drag force was studied.

Fig.2 illustrates the test results. Model sandy ground was of a range of density. The drag force increased with the pipe velocity, revealing a viscous nature of sand. The intensity of viscosity increased with the density of sand. Although the true mechanism of the viscosity is not known yet, the use of the viscosity term in Eq.7 appears to be reasonable.

ON RESIDUAL STRENGTH OF LIQUEFIED SAND

The residual strength of liquefied sand was needed to be studied as well. The residual strength at large shear deformation under undrained conditions has been studied by many people (e.g., Poulos et al., 1984; Ishihara, 1993) and it is to date known that the denser sand has the greater strength. However, those studies have been made by running laboratory element tests such as a triaxial one. It is important, however, that there are many differences between laboratory element tests and a shaking liquefied ground. The present study mentions two of them among others; the existence of inertia force induced by seismic acceleration and the effects of seepage force.

The differences mentioned above can be quantitatively studied to a certain extent by examining the results of model shaking tests (Toyota and Towhata, 1994). Unless the involved sand was very loose, the lateral motion of liquefied model ground stopped when excess pore water pressure was still high and the ground surface was inclined, (Fig.3). The cease of motion as observed at an inclined configuration took place because the sand maintained some shear strength.

The closed-form solution of the ultimate displacement (Towhata et al., 1992) already considered the effects of residual strength of liquefied sand. This solution was applied to interpret the present model tests in order to assess the strength of sand. The results of this assessment is indicated in Fig.4 by hollow symbols. Since the ultimate surface slope was greater when the sand was denser, the residual strength at the ultimate displacement is greater as well for denser materials.

In contrast to the impact-shaking tests as mentioned above, several model tests were carried out by continuously shaking the ground until the ultimate displacement was achieved. It was therein observed that the ground surface became level, irrespective of the sand density. Consequently, the sand strength assessed from these tests is negligible as indicated by solid symbols in Fig.4.

The effects of shaking demonstrated in Fig.4 were further studied by model-pipe tests in which a model pipe moved in the horizontal direction cyclically in a liquefied Toyoura sand. Similar to Fig.3, the drag force required for a pipe movement (10mm/sec.) was recorded together with the pipe displacement and the excess pore water pressure. Fig.5 indicates a case where the void ratio was 1.05 and the model ground was shaken by 500gal input motion with 3.5 Hz. The relationship between the drag force and the pipe displacement is qualitatively equivalent to the stress-strain behavior of tested sand, whilst the diagram of force vs. pore pressure suggests the shape of a stress-path diagram.

The force-displacement diagram in Fig.5 reveals a clear difference in the drag force during and after shaking. When shaking was going on, the magnitude of the force was held small, although fluctuating to some extent due to the inertia force. After the shaking was turned off,

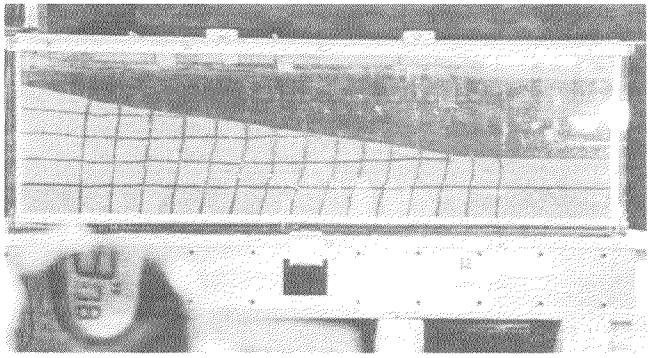

(a) Case with e=0.95

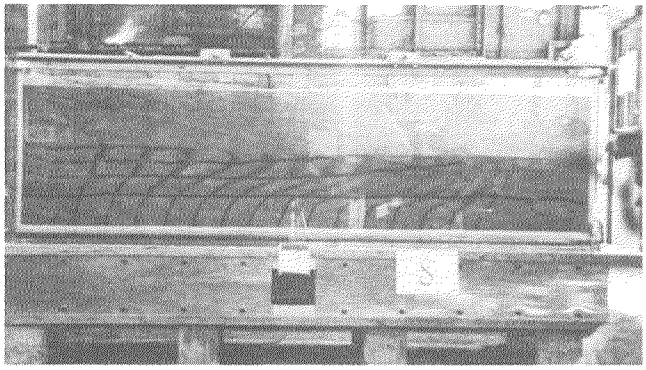

(b) Case with e=1.03 (very loose)

Fig.3 Configuration at the end of flow.

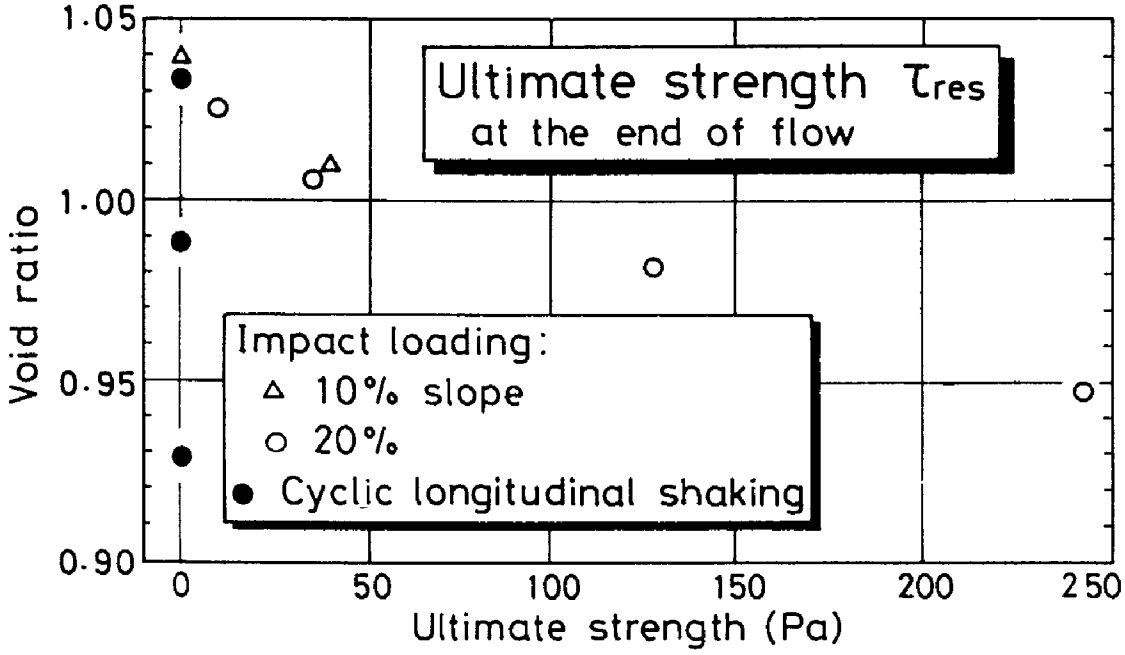

Fig.4 Variation of residual strength with sand density.

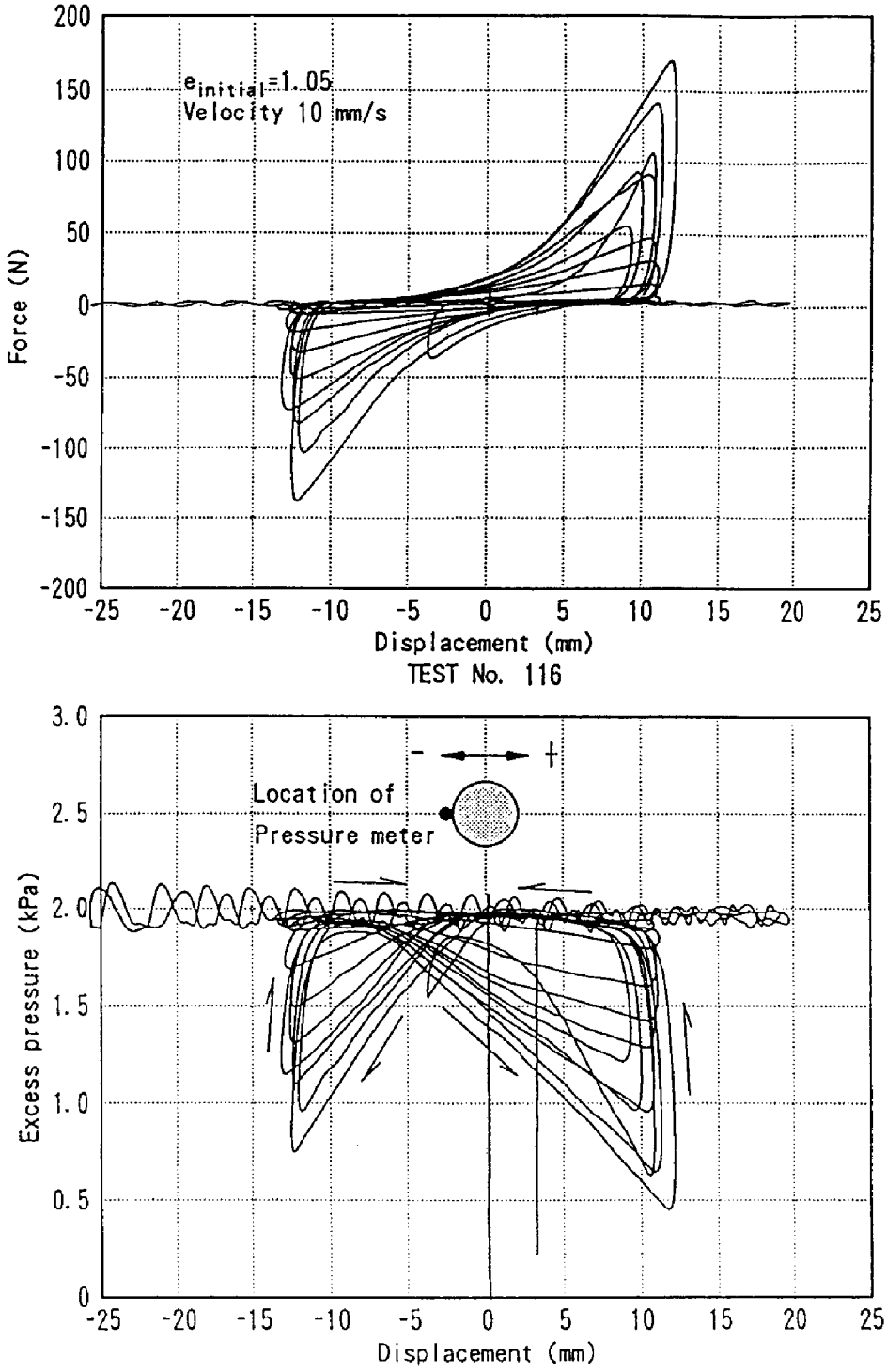

Fig.5 Model pipe test in liquefied ground.

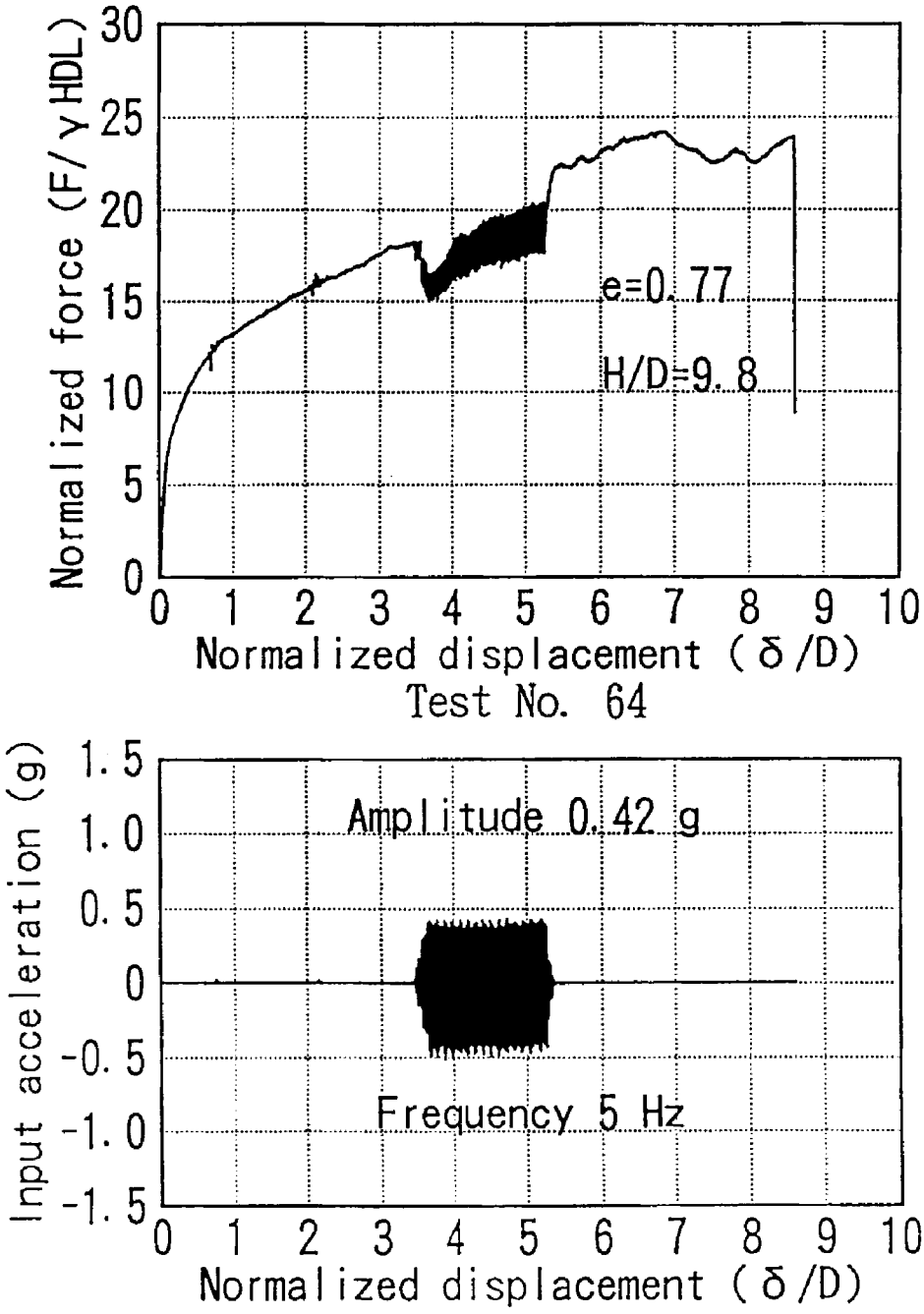

Fig.6 Model pipe test in dry sand.

on the contrary, the amplitude of the force started to be larger. The observed shape of the force-displacement curve is very similar to the undrained stress-strain behavior of loose sand.

Moreover, the variation of excess pore water pressure with displacement (Fig.5) indicates the effects of shaking similarly. In the course of shaking, the excess pore water pressure was held high and constant, indicating 100% development of liquefaction. After the end of shaking, in contrast, a temporary reduction of pore pressure towards the maximum displacement was observed. This behavior is similar to the undrained stress path diagram in which a dilatancy of grain packing induces a reduced pore pressure upon stress loading.

The reason of the difference as stated above is speculated below. The dilatancy of granular packing occurs when a sand grain is pushed by an intergranular force towards an adjacent grain. Sliding up along the surface of the second grain leads to the overall expansion of sand. When undrained, sand cannot absorb water from outside and cannot compensate for the dilatancy of packing. Consequently, the excess pore water pressure drops and the effective stress develops; thus increasing the shear stiffness. When the inertia force is superimposed upon sand during shaking, the intergranular contact force fluctuates in a very complex manner and the state of dilatant particle contact is easily destroyed. Thus, a drop of pore pressure is not necessary very much and the effective stress does not develop.

The idea of destroyed particle contact is further studied by pipe test performed in a dry sand deposit. A pipe embedded in a dry Toyoura sand (e=0.760) was pulled laterally at a rate of 4mm/sec. in a similar manner as in Fig.5. Since the sand was dry, no excess pore water pressure developed. Initially, the pipe was moved in a monotonic manner without shaking. The drag force increased with the displacement, indicating the subgrade reaction of model ground. At sometime, a lateral shaking started and the drag force decreased in magnitude. When the shaking was switched off later, the drag force came back to the extrapolation of the original loading curve. Thus, the drag force or the sand stiffness was reduced only during shaking. This observation suggests that the particle contact pressure which mainly generates the sand stiffness was destroyed to some extent by the induced cyclic inertia force.

EXAMPLE ANALYSES

Eq.7 was applied to several cases in model and insitu situations. The ultimate displacement was calculated first and then the time history of λ was obtained so that the time development of displacement, u, was calculated. The residual strength needed for analysis was determined by using Fig.4, in accordance with the static and shaken conditions. Since much is not known yet about the viscosity of liquefied sand, the viscosity coefficient, c, in Eq.7 was determined to make the critical damping equal to 0.62. Note that this value of damping ratio is equal to the one of a rigid-plastic material (see Fig.7).

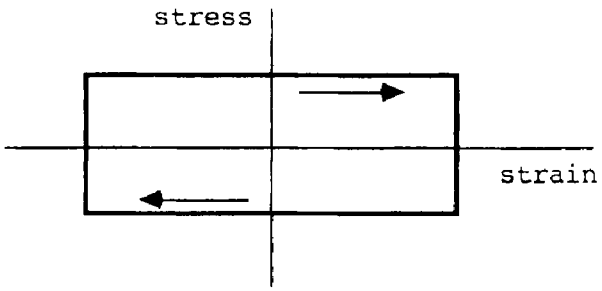

Fig.7 Rigid-perfectly plastic stress-strain curve.

Fig.8 illustrates the calculated displacement of a model ground with a variety of density. Since the flow occurred under static gravity, the residual strength under static conditions in Fig.4 was employed. The observed displacement as well as the size of the ground is demonstrated in Fig.9 See that the duration time of flow is independent of sand density or the magnitude of displacement in both calculation and observation.

Fig.10 indicates the displacement when the motion occurred under sustained shaking. The

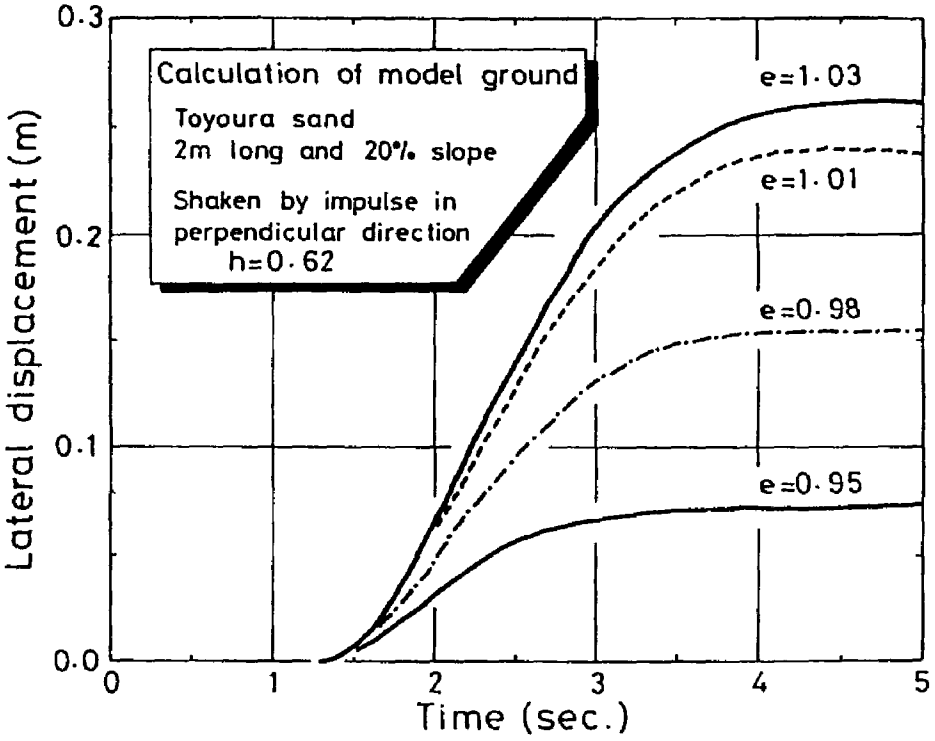

Fig.8 Calculated time history of model slope under static gravity.

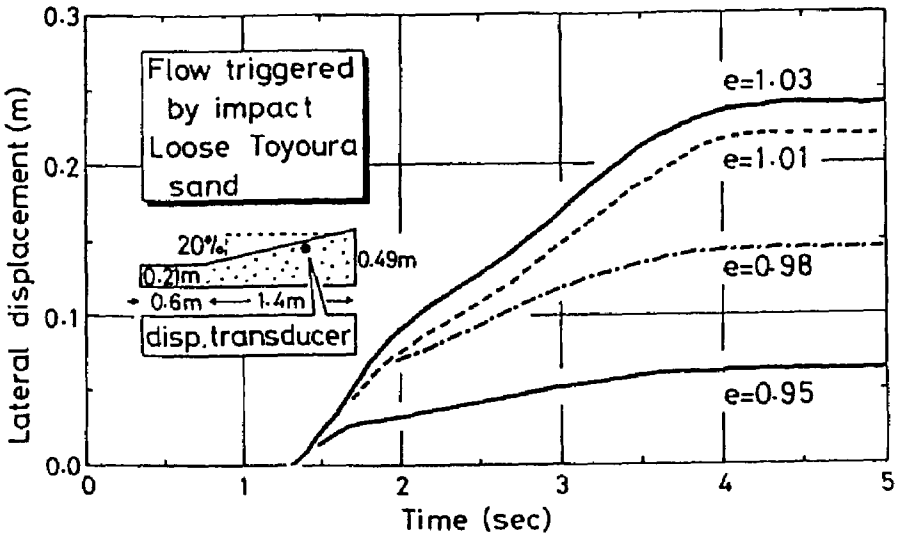

Fig.9 Observed time history of model slope under static gravity.

385

residual strength was set equal to zero as revealed in Fig.4. The viscosity was again determined to make the critical damping ratio equal to 0.62. Consequently, a good agreement between calculation and observation was achieved.

Fig.11 compares the prediction and calculation of a displacement in Noshiro City where a substantial ground displacement occurred at the time of the 1983 Nihonkai-Chubu earthquake. Since no earthquake motion was recorded at this site, a harmonic base motion of 150 gals and 2 Hz were assumed to continue for 10 seconds after the onset of subsoil liquefaction. During this shaking, the residual strength was set equal to zero and λ equal to about 0.75 was attained at the end of shaking. Since a greater strength was needed under static conditions after this time, the movement could not develop further. Hence, the ultimate deformation as obtained previously (Towhata et al., 1992) was multiplied by λ=0.75, and the displacement illustrated in Fig.11 was obtained. There appears to be a good agreement between calculation and observation by Hamada et al. (1986).

CONCLUSION

An attempt was made to develop an analytical measure to predict the time history of lateral ground movement induced by seismic liquefaction. The lack of knowledge about nature of soil undergoing lateral flow and large deformation was compensated for by running several model shaking tests. Accordingly, the following conclusions were drawn;

(1) An application of the theory of Lagrangean equation of motion made it possible to derive a single-degree-of-freedom equation of motion that is easy to solve.
(2) This equation of motion includes a viscosity term and the residual strength of liquefied sand.
(3) Model tests indicated that the resistance of liquefied sand against lateral movement of an embedded pipe is affected by the rate of pipe movement. Hence, there is a viscous nature in liquefied sand.
(4) Dilatancy of sand that could develop negative pore pressure and shear resistance against large distortion is destroyed by seismic inertia force. Hence, liquefied sand during shaking is of negligible shear strength.
(5) Sand loses strength during shaking even when it is dry.
(6) The residual strength starts to occur after shaking.
(7) It is possible to obtain a good agreement between calculation and observation.

ACKNOWLEDGMENT

The model tests described in this text were conducted by Mr.W.Vargas and Mr.M.Yao. Their contribution is deeply appreciated by the authors.

REFERENCES

Hamada,M., Yasuda,S., Isoyama,R., and Emoto,K. (1986) "Generation of Permanent Ground Displacements Induced by Soil Liquefaction," Proc. JSCE, 1986. No.376/III-6, pp.211-220.

Ishihara,K (1993) "Liquefaction and Flow Failure during Earthquakes," Geotechnique, 1993. Vol.43, No.3, pp.351-415.

Poulos,S.J., Castro,G. and France,J W. (1984) "Liquefaction Evaluation Procedure," Proc. ASCE, Vol.111, GT6, pp.772-792.

Towhata,I. Sasaki,Y., Tokida,K., Matsumoto,H., Tamari,Y. and Yamada,K. (1992) "Prediction of Permanent Displacement of Liquefied Ground by Means of Minimum Energy Principle." Soils and Foundations, Vol.32, No.3, pp.97-116.

Toyota,H. and Towhata,I. (1994) "Post-liquefaction Deformation of Cohesionless Soils," Proc. 5th US-Japan Workshop on Earthquake Resistant Design of Lifeline Facilities and Counter-Measures against Soil Liquefaction.

Vargas-Monge,W (1994) "Study on Flowing Liquefied Ground by Means of Model Pipe Tests", Master thesis, University of Tokyo.

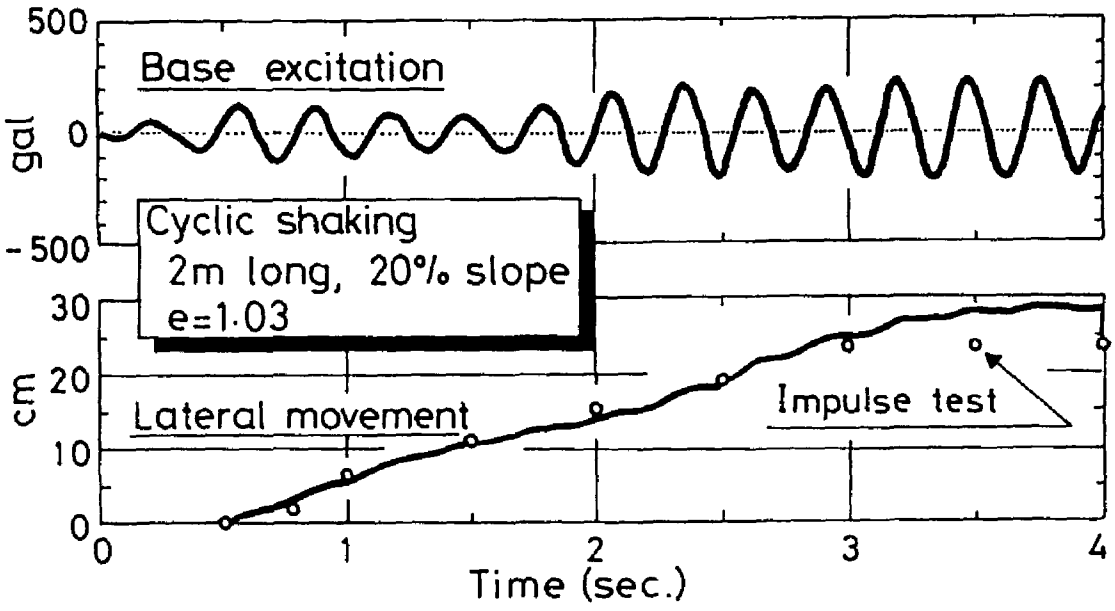

Fig.10 Displacement of slope undergoing shaking.

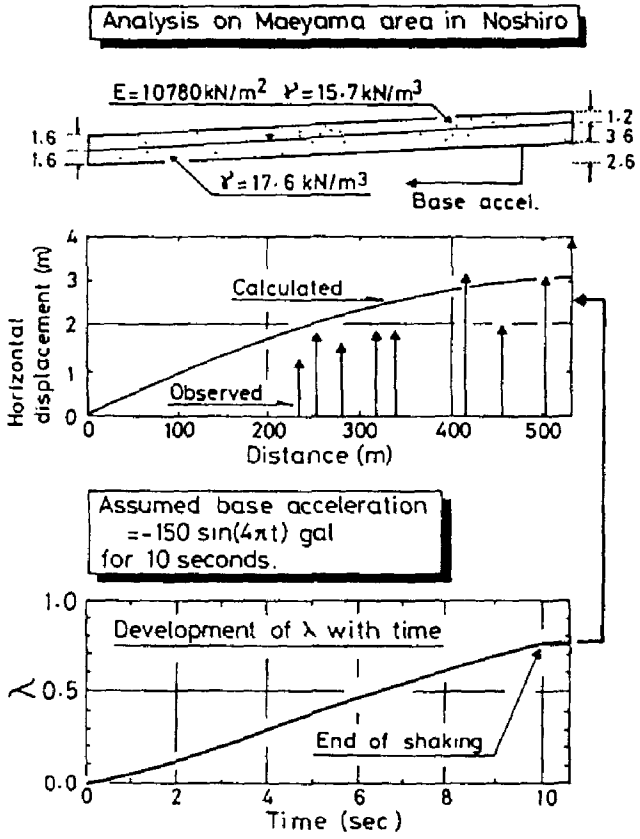

Fig.11 Calculated and observed displacement in Noshiro City.